Acta Biochim Biophys Sin 2014, 46: 957–964 | © The Author 2014. Published by ABBS Editorial Office in association with Oxford University Press on behalf of the Institute of Biochemistry and Cell Biology, Shanghai Institutes for Biological Sciences, Chinese Academy of Sciences. DOI: 10.1093/abbs/gmu093.
Advance Access Publication 29 September 2014

Original Article

Four residues of propeptide are essential for precursor folding of nattokinase

Yan Jia[1], Xinhua Cao[2], Yu Deng[2], Wei Bao[2], Changyan Tang[2], Hanjing Ding[2], Zhongliang Zheng[2]*, and Guolin Zou[2]*

[1]Beijing Key Laboratory of Plants Resource Research and Development, School of Science, Beijing Technology and Business University, Beijing 100048, China
[2]State Key Laboratory of Virology, Department of Biochemistry and Molecular Biology, College of Life Sciences, Wuhan University, Wuhan 430072, China
*Correspondence address. Tel: +86-27-87645674; Fax: +86-27-68752560; E-mail: zouguolin@whu.edu.cn

Subtilisin propeptide functions as an intramolecular chaperone that guides precursor folding. Nattokinase, a member of subtilisin family, is synthesized as a precursor consisting of a signal peptide, a propeptide, and a subtilisin domain, and the mechanism of its folding remains to be understood. In this study, the essential residues of nattokinase propeptide which contribute to precursor folding were determined. Deletion analysis showed that the conserved regions in propeptide were important for precursor folding. Single-site and multi-site mutagenesis studies confirmed the role of Tyr10, Gly13, Gly34, and Gly35. During stage (i) and (ii) of precursor folding, Tyr10 and Gly13 would form the part of interface with subtilisin domain. While Gly34 and Gly35 connected with an α-helix that would stabilize the structure of propeptide. The quadruple Ala mutation, Y10A/G13A/G34A/G35A, resulted in a loss of the chaperone function for the propeptide. This work showed the essential residues of propeptide for precursor folding via secondary structure and kinetic parameter analyses.

Keywords intramolecular chaperone; propeptide; subtilisin; essential residues; nattokinase

Received: July 2, 2014 Accepted: August 28, 2014

Introduction

When the Anfinsen's dogma was presented, it was assumed that the protein structure is determined by the protein's amino acid sequence [1]. However, the proper folding of some proteins requires the assistance of molecular chaperones, while the folding of other proteins requires their intramolecular chaperone (IMC) [2]. The discovery that an IMC plays a crucial role in protein folding that leads to a functionally active conformation was based on studies of proteases, such as subtilisin [3], α-lytic protease [4], and carboxypeptidase Y [5]. Unlike molecular chaperone, the IMC is encoded in the primary sequence of the protein and is usually termed a propeptide. Although it is not part of the functional domain and does not contribute to protein function, it helps the protein to form an active 3D structure [6].

The propeptide can function as a template that imparts structural information to the subtilisin domain during precursor folding *in vivo* and *in vitro* [7,8]. Therefore, point mutations within the propeptide can alter the structure and activity of subtilisin, even though the mutation is not a part of the subtilisin domain. Because some human diseases are caused by protein-memory mutation [9], it is important to decipher the precise roles of an IMC in protein folding. In particular, it is important to note that mutations in the IMC can cause misfolding of the functional domain, resulting in distortion of their function and leading to human diseases, even if the primary structures of the functional domains are identical.

The refolding pathway of subtilisin E *in vitro* was reported by Yabuta *et al*. [3]. Propeptide-mediated protein folding mechanism in subtilisin was established as following stages: (i) the protease's folding mediated by its cognate propeptide; (ii) the autoprocessing of the peptide bond between the propeptide and subtilisin, which results in structural reorganization; and (iii) the propeptide's degradation, which locks the protease into a stable conformation [10]. The crystal structures of the propeptide–subtilisin complexes have been determined from subtilisin SBT-70 [11] and subtilisin E [12]. Evidence has revealed that these two structures represent the propeptide–subtilisin complex at the beginning of the stage (iii) when structural reorganizations are finished. However, the interaction information between the propeptide and subtilisin domains during stages (i) and (ii) is still unknown. In addition, it seems difficult to study this interaction from the determined structure of propeptide–subtilisin complex. Therefore, it may be an approach to focus on the conserved residues of propeptide.

Nattokinase (NK) is synthesized as a precursor, which consists of a signal peptide, a propeptide, and a subtilisin domain. The 77-residue propeptide at the N-terminal end of

subtilisin assists in the folding of its cognate subtilisin domain and is termed as an IMC. Two 3D models of NK [13] and the propeptide–NK complex [7] were previously constructed. Site-directed mutagenesis and molecular dynamic simulations were used to probe the importance of the hydrogen bonds around the active site of NK [14]. In addition, our earlier study demonstrated that specific interactions between the propeptide and subtilisin domain are important for the precursor folding, and conserved regions of the propeptide may be involved in the interactions [7,15]. Thus, certain residues in the conserved regions of the propeptide play an essential role during the precursor folding, and it is likely that these substitution mutations lead to defects in the production of active subtilisin during the precursor folding. The determination of such residues in the propeptide will further facilitate elucidation of the IMC-mediated protein folding mechanism.

NK is a potent fibrinolytic enzyme from *Bacillus subtilis natto* and was first found in the traditional Japanese soybean food natto [16]. Recently, the non-hydrogen NK structure was determined at 1.74 Å resolution, which was carried out by cultivating *B. subtilis* natto in deuterated medium [17]. NK has potent fibrinolytic activity, dissolves fibrin directly, and enhances the production of both plasmin and other clot-dissolving agents, including urokinase. Therefore, NK is a promising agent that can be administered orally for thrombolytic therapy. In addition, its activity is enhanced in the plasma, leading to a longer half-life with oral administration [18]. The mutation of some essential residues may improve the properties of NK to broaden its use in medical applications.

Here, the relationship was described between the crucial residues of the propeptide and the secondary structure and the catalytic efficiency of subtilisin. This is a report to determine four essential residues during precursor folding *in vivo* of the precursor, via secondary structure and kinetic parameter analyses.

Materials and Methods

Materials

The substrate succinyl-Ala-Ala-Pro-Phe-*p*-nitroanilide (suc-AAPF-pNA) was purchased from Sigma (St Louis, USA). The BCA protein assay reagent kit was obtained from Pierce (Rockford, USA). The Ni-NTA column was obtained from Invitrogen (Carlsbad, USA), and the DEAE-Sepharose Fast Flow column was purchased from Amersham Biosciences (San Francisco, USA). Polyvinylidene difluoride (PVDF) and enhanced chemiluminescence western blotting detection reagents were obtained from Millipore Corporation (Billerica, USA).

B. subtilis var. *natto* was used as the source of genomic DNA. *Escherichia coli* BL21(DE3) was the host bacterial strain for the pET-26b(+) vector expression system. The gene encoding the precursor NK (propeptide and mature protease) was inserted into the plasmid pET-26b(+) as described previously [7].

Production of residue-truncated propeptide and site-directed mutagenesis

Residue-truncated propeptide single-site and multi-site mutagenesis were performed by the overlap extension method [19]. All the precursor genes were confirmed by DNA sequencing.

Protein expression, purification, and measurement

The recombinant plasmids were introduced into *E. coli* strain BL21(DE3) [20] and transformants were grown in Luria–Bertani broth supplemented with 50 μg/ml kanamycin. When the absorbance at 600 nm (A_{600}) reached 1.0, the gene expression was induced by adding isopropyl-1-thio-β-D-galactopyranoside (final concentration of 0.7 mM). After 20 h at 20°C, the cells were harvested by centrifugation and washed twice with a wash buffer containing 50 mM NaH_2PO_4 and 300 mM NaCl, pH 8.0. The cells were resuspended in washing buffer and then disrupted by sonication on ice. The suspension was centrifuged at 10,000 *g* for 1 h at 4°C, and the supernatant was used for purification conducted at 4°C. Proteins were purified by column chromatography using a Ni-NTA column and a DEAE-Sepharose Fast Flow column. After purification to homogeneity, the protein concentration was determined using the BCA protein assay reagent kit.

Sodium dodecyl sulfate–polyacrylamide gel electrophoresis and immunoblot analysis

Sodium dodecyl sulfate–polyacrylamide gel electrophoresis (SDS–PAGE) was performed using a 12% (w/v) polyacrylamide separating gel with a 5% (w/v) stacking layer according to the procedure of Laemmli [21].

For immunoblotting, the proteins separated by SDS–PAGE were electrically transferred onto a PVDF membrane. Membranes were soaked in blocking buffer (5% non-fat dry milk) overnight at 4°C and then incubated with mouse anti-His-tag monoclonal antibody at 37°C for 1.5 h, followed by horseradish peroxidase-conjugated goat anti-mouse IgG (H+L) at 37°C for 45 min. Detection was performed using enhanced chemiluminescence western blotting detection reagents.

Determination of kinetic parameters

Kinetic parameters were measured using the chromogenic substrate suc-AAPF-pNA in 10 mM phosphate-buffered saline (PBS), pH 8.0, and 4% (v/v) dimethyl sulfoxide (DMSO) [22] in a final volume of 0.25 ml. The reaction was initiated by the addition of the enzyme. The absorbance of the *p*-nitroaniline produced during the incubation was measured at 405 nm. Enzyme concentrations were determined to

permit calculation of the turnover number (k_{cat}) from the relationship $k_{cat} = V_{max}$/[enzyme]. The Michaelis–Menten constant (K_m) and V_{max} values were determined from the initial rate measurements of suc-AAPF-pNA hydrolysis.

Circular dichroism studies

All circular dichroism (CD) measurements were conducted using a J-810 automatic spectropolarimeter (Jasco, Tokyo, Japan). The spectra were measured over a wavelength range of 260 to 190 nm using a 1 mm pathlength cell. The concentration of purified proteins was maintained at 100 μg/ml. All spectral measurements were performed in 10 mM PBS, pH 7.0. Each spectrum is an average of three scans. The α-helical content of proteins was calculated by analyzing the spectrum [23].

Fluorescence measurements

Fluorescence measurements were performed using an F-4500 fluorescence spectrometer (Hitachi, Tokyo, Japan). The purified proteins were excited at 295 nm, and the emission was monitored from 300 to 500 nm. The protein concentrations were maintained at 10 μg/ml. Each spectrum is an average of three scans.

Results

Sequence alignments among subtilisin propeptides

Comparison of the amino acid sequence of the NK propeptide with those of several different subtilisins revealed that the overall sequence identity is low, but three regions (Tyr10–Lys15, Gly34–Ala46, and Leu59–Asp71) displayed significant sequence conservation (**Fig. 1**).

From the propeptide–subtilisin complex structure [7], the propeptide domain is made up of four antiparallel β-strands (named β-strand I, II, III, and IV, containing residues Lys8–Lys15, Gly34–Phe41, Asn45–Leu51, and Ser64–Ala74, respectively) and two α-helices (formed by Ser23–Lys33 and Glu53–Lys60). In addition, β-strands are formed by conserved regions and two α-helices are formed by non-conserved segments.

Conserved regions within the propeptide for precursor folding *in vivo*

Previous studies [7] have shown that the propeptide of NK functions as an IMC that helps the folding of the subtilisin domain *in vivo*. The conserved regions may be critical for this process. In this study, to determine whether the conserved regions of the propeptide are important for folding, a mutant without 9 N-terminal amino acids (ΔN9) and a mutant without 15 N-terminal amino acids (ΔN15) were produced and their secondary structures and kinetic parameters of these mutants were measured. The secondary structure (**Supplementary Fig. S1**) and kinetic parameters (**Table 1**) of the ΔN9 mutant were almost the same as those of wild-type (WT) subtilisin. After protein purification, ΔN15 was not obtained due to the low yield. However, the crude extracts of ΔN15 showed weak subtilisin activity using the chromogenic substrate suc-AAPF-pNA (data not shown), and there were precursor band and mature protein band for ΔN15 in western blotting (**Fig. 2B**).

The region from Tyr10 to Lys15 belongs to β-strand I of conserved region, whereas the region from Ala1 to Lys9 is a non-conserved segment. These results suggested that the conserved regions of the propeptide are important for the precursor folding *in vivo*.

The effect of single-site mutants on precursor folding

Previous study indicated that the importance of residue is consistent with residue conservation, it was expected that these conserved hydrophobic residues of the propeptide would be responsible for precursor folding [7]. As shown in **Fig. 1**, the hydrophobic amino acids Tyr10, Gly13, Gly34, Gly35, and Pro63 in the three conserved regions are identical among different subtilisins. Single and combinational site-directed mutagenesis of these residues to Ala were performed, respectively. Secondary structures and kinetic parameters of recombinant propeptide mutants were measured.

After purification to homogeneity (**Fig. 2A**), secondary structures of these proteins were analyzed using CD (**Fig. 3A,C**) and fluorescence studies (**Fig. 3B,D**). As shown in **Fig. 3A,C**, CD measurements indicated that Y10A, G13A, and G35A had different secondary structures from

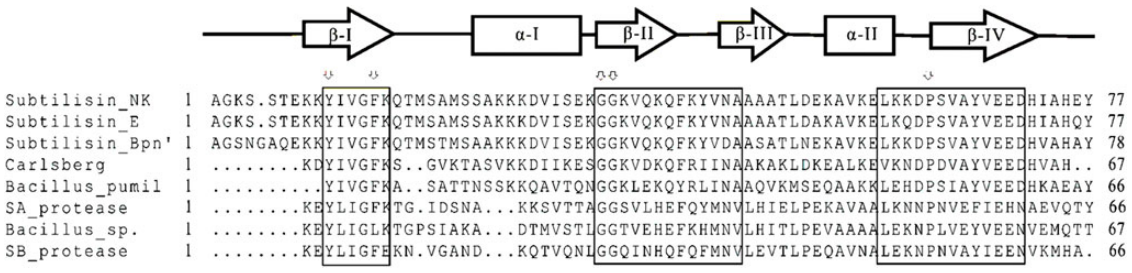

Figure 1. Sequence alignment of propeptides from various subtilisins showing three conserved regions Amino acids in squares represent conserved residues, and the ranges of the secondary structures are indicated. The identical residues in conserved regions are indicated by arrows.

Table 1 Kinetic constants[a] and α-helix contents of WT subtilisin and mutants

Enzymes	k_{cat} (S^{-1})	K_m (μM)	k_{cat}/K_m (S^{-1} mM^{-1})	α-helix content (%)
WT	8.26 (±0.51)	155 (±4)	53.3	36.30
ΔN9	8.15 (±0.36)	159 (±3)	51.3	36.06
Y10A	0.80 (±0.06)	137 (±3)	5.83	41.68
G13A	1.53 (±0.14)	178 (±4)	8.60	39.66
G34A	3.79 (±0.23)	134 (±2)	28.3	36.63
G35A	1.35 (±0.12)	167 (±3)	8.08	49.74
P63A	8.33 (±0.36)	174 (±5)	47.9	36.97
Y10A/G35A	0.013 (±0.003)	1.22 (±0.03)	0.0107	17.81

[a]Kinetic constants were measured with the chromogenic substrate suc-AAPF-pNA in 10 mM phosphate buffer, pH 8.0, 4% (v/v) DMSO at (25 ± 0.2)°C.

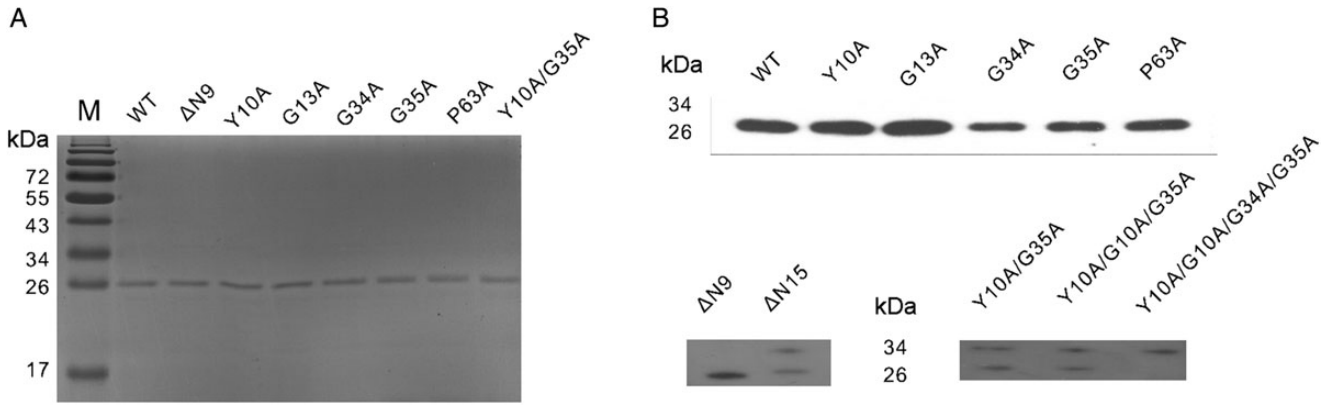

Figure 2. The purification of WT subtilisin and mutants (A) SDS−PAGE analysis of purified WT subtilisin and mutants. Purified proteins were applied to a 12% polyacrylamide gel, and after electrophoresis, the gel was stained with Coomassie Brilliant Blue. Protein standards (in kilodaltons) were applied. (B) Western blot analysis of purified WT subtilisin and mutants. Protein standards (in kilodaltons) were applied.

that of WT subtilisin, whereas the secondary structures of G34A and P63A were only slightly different and almost identical, respectively, to that of WT subtilisin. This is in accordance with the fluorescence study results (**Fig. 3B,D**). The mutation causes a blue shift in the fluorescence maxima of Y10A, G13A, G34A, and G35A, with a simultaneous decrease in the fluorescence intensity. However, the spectrum of P63A was similar to that of WT subtilisin. These results showed that Y10A, G13A, and G35A had different secondary structures from that of WT subtilisin, whereas the secondary structures of G34A and P63A were only slightly different from WT subtilisin.

As shown in **Table 1**, the catalytic efficiencies (k_{cat}/K_m) of Y10A, G13A, and G35A were reduced ~10 folds whereas that of G34A was ~2 folds less compared with WT subtilisin. However, there was just a slight decrease in the catalytic efficiency (k_{cat}/K_m) of P63A compared with WT subtilisin. The results of kinetic analysis were in accordance with the secondary structure analyses.

These results indicated that the hydrophobic residues Tyr10, Gly13, and Gly35 are the most important amino acids in the conserved regions for precursor folding and that Gly34 cooperatively contributed to precursor maturation. However, Pro63 had no significant contribution to precursor folding.

Characterization of the secondary structures and kinetic parameters of multi-site mutants

To determine whether there is cooperation among the important residues (Tyr10, Gly13, Gly34, and Gly35) of the conserved regions during the precursor folding, the multi-site mutants Y10A/G35A, Y10A/G13A/G35A, and Y10A/G13A/G34A/G35A were produced and the secondary structures and kinetic parameters of these mutants were determined.

After protein purification (**Fig. 2A**), the secondary structure of Y10A/G35A was determined by CD (**Fig. 4A**) and fluorescence studies (**Fig. 4B**). **Figure 4** showed that Y10A/G35A had a different secondary structure from that of WT subtilisin. The double mutation caused a blue shift in the fluorescence maxima and a simultaneous decrease in the fluorescence intensity. As shown in **Table 1**, Y10A/G35A

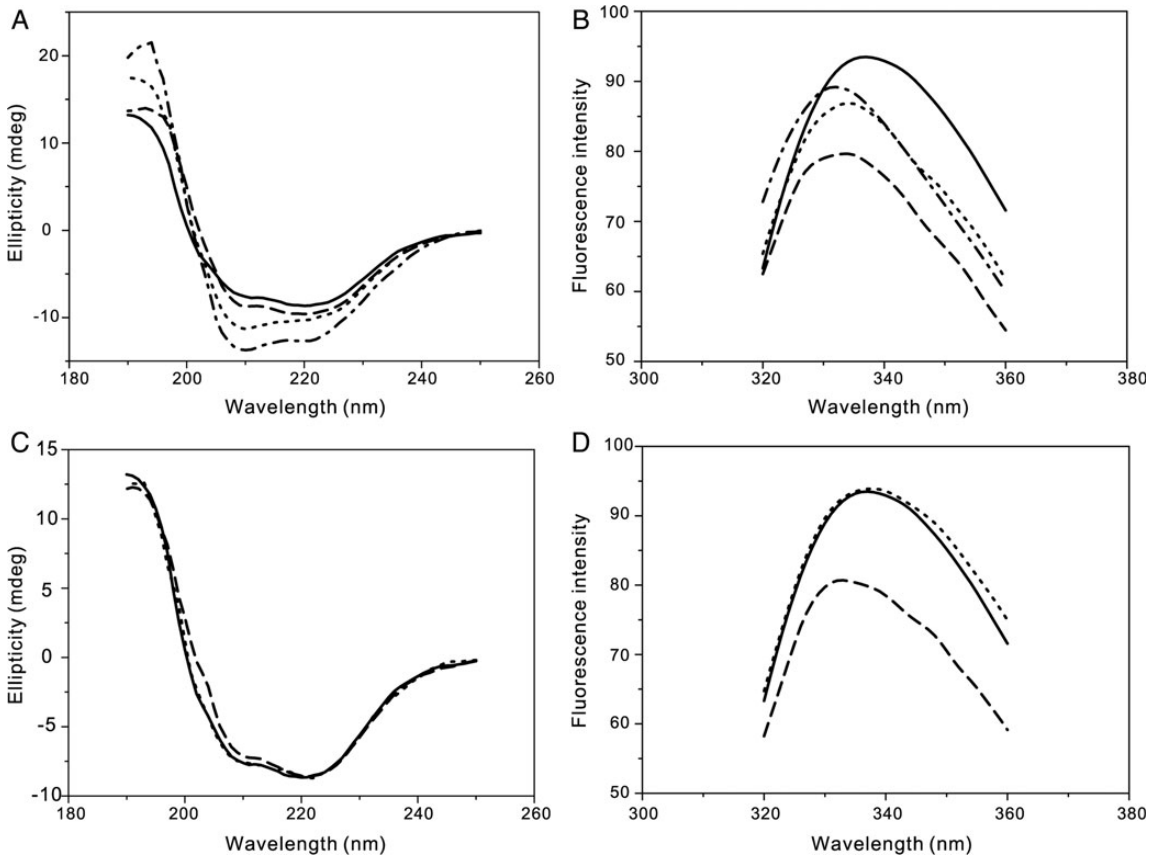

Figure 3. CD spectra and intrinsic fluorescence emission spectra of WT subtilisin and single-site mutants In (A) and (B), the WT subtilisin is represented by a solid line, Y10A is represented by a dotted line, G13A is represented by a dashed line, and G35A is represented by a dashed and dotted line. In (C) and (D), the WT subtilisin is represented by a solid line, P63A is represented by a dotted line, and G34A is represented by a dashed line. On CD spectra measurement, a concentration of 0.1 mg/ml was used for all proteins. For intrinsic fluorescence emission spectra measurement, the final concentration of each protein was 10 μg/ml, and the excitation wavelength used was 295 nm.

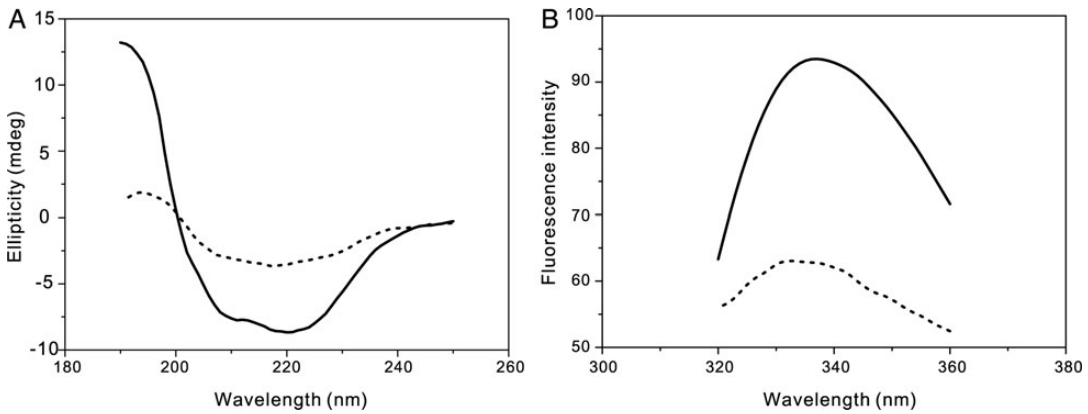

Figure 4. The spectra of the WT subtilisin and mutants (A) CD spectra of WT subtilisin and Y10A/G35A. A concentration of 0.1 mg/ml was used for proteins. (B) Intrinsic fluorescence emission spectra of the WT subtilisin and mutants. The final concentration of each protein was 10 μg/ml, and the excitation wavelength was 295 nm. The WT subtilisin is represented by a solid line, Y10A/G35A is represented by a dotted line. Data were collected as described in the Materials and Methods section.

reflected a reduction of 3–4 orders of magnitude in catalytic efficiency. The Y10A/G13A/G35A mutant was not obtained due to low yield. However, the crude extracts showed weak subtilisin activity towards the chromogenic substrate suc-AAPF-pNA (data not shown). In **Fig. 2B**, the bands of precursor and mature protein (ΔN9, ΔN15, Y10A/G35A, Y10A/G13A/G35A, and Y10A/G13A/G34A/G35A) were compared in a gel (western blotting of bacterial liquid).

There was no precursor band for ΔN9, and no mature protein band for Y10A/G13A/G34A/G35A.

These results indicated that the folding of ΔN9 was successful, the folding of Y10A/G13A/G34A/G35A was blocked, and the folding of ΔN15, Y10A/G35A, and Y10A/G13A/G35A were influenced due to the weakened processing activity.

Discussion

In this study, we investigated the processing of the NK precursor *in vivo*. Crucial residues (Tyr10, Gly13, Gly34, and Gly35) of the subtilisin propeptide were determined during precursor folding *in vivo*. This knowledge could further facilitate elucidation of the IMC-mediated protein folding mechanism. Although NK was analyzed as a model, it is likely that similar mechanisms exist for all subtilisins.

Based on our 3D models, the structure of NK alone has the same root-mean-square value of 0.28 Å as the NK–propeptide complex (**Fig. 5**). This is also in accordance with other subtilisins. According to the crystal structures of subtilisin SBT-70 [11] and subtilisin E [12], the subtilisin SBT-70 complex was formed by the addition of a separately produced propeptide domain, and the subtilisin E complex was refolded. These two structures have the same root-mean-square value of 0.44 Å [12]. The structure of NK alone clearly fits well with these subtilisin domains in the complex.

Sequence alignments among different subtilisins revealed that three regions, Tyr10–Lys15, Gly34–Ala46, and Leu59–Asp71, displayed significant amino acid sequence conservation. The folding of ΔN9 was successful, and the folding of ΔN15 was influenced due to the weakened processing activity. These results suggested that the conserved regions of the propeptide are important for the precursor folding.

The hydrophobic residues Tyr10, Gly13, Gly34, Gly35, and Pro63 in the three conserved regions are highly conserved. As it was expected that these hydrophobic residues in the propeptide would be responsible for precursor folding, single-site mutants and multi-site mutants were constructed. The results indicated that the hydrophobic residues Tyr10, Gly13, and Gly35 are the most important amino acids in the conserved regions for precursor folding and that Gly34 cooperatively contributed to precursor maturation. However, Pro63 had no significant contribution to precursor folding.

Tyr10 and Gly13 are located in β-strand I that form the interface of propeptide–subtilisin complex (**Fig. 6**). Mutation to Ala would alter the interfacial interactions between the two domains, directly leading to the structural alterations of two α-helices of subtilisin domain. Trp106 and Trp113 are on one of the α-helices, and they play a significant role in fluorescence spectrum and subtilisin activity in subtilisin E [24]. In addition, W106Y, W113Y, and W106Y/W113Y all show blue shifts in fluorescence spectra [24]. Therefore, mutation of Gly13 to Ala would cause the alteration of Trp106 and Trp113 that leads to a blue shift in fluorescence spectra.

Gly34 and Gly35 are on the starting of β-strand II that interacts with the two α-helices formed by the subtilisin domain (**Fig. 6**). Mutation of Gly35 with Ala causes an additional hydrogen bond formed by the O of Ile30 and the N of Ala35 (**Supplementary Fig. S2**). Ile30 is involved in the formation of one α-helix which would stabilize the structure of propeptide, and it is important for precursor folding of subtilisin E [8]. Simultaneously, substitution of Gly34 and

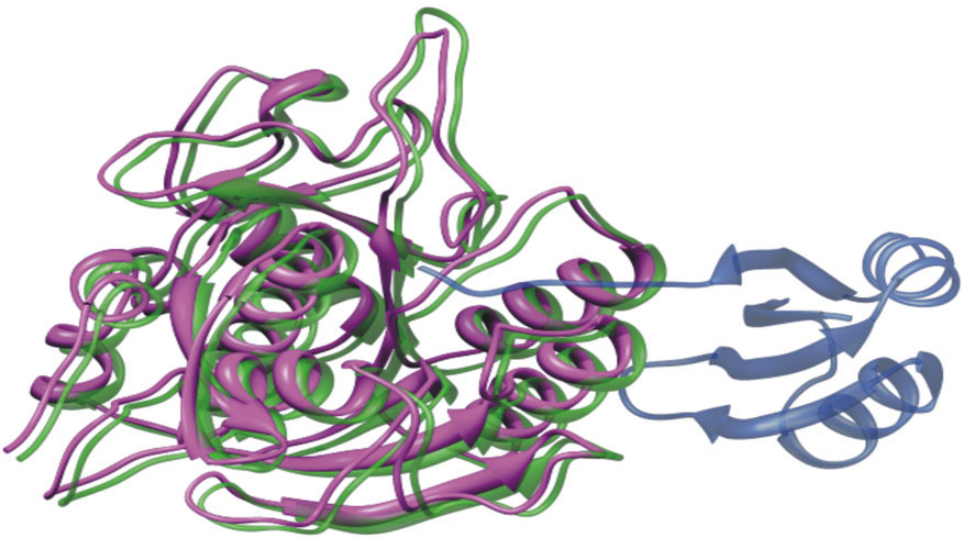

Figure 5. The structure of propeptide–subtilisin complex overlapped by that of mature subtilisin The structure of subtilisin and that in the complex give a root-mean-square value of 0.28 Å.

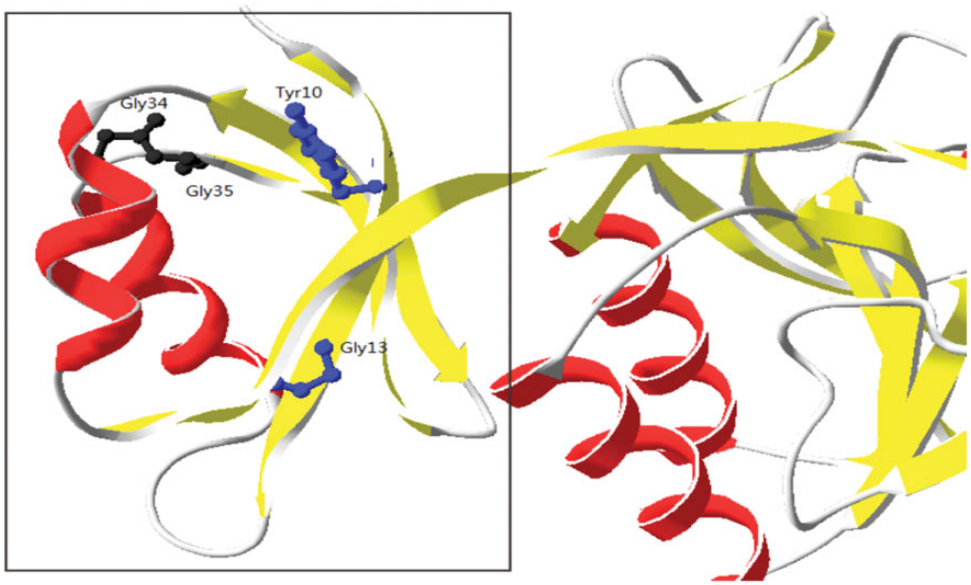

Figure 6. The structure for propeptide and the interface between propeptide and subtilisin domains Propeptide are displayed in square. On the propeptide, Tyr10, Gly13, Gly34, and Gly35 are labelled by residue name.

Gly35 with Ala would disturb the interactions between β-strand II of propeptide and α-helices of subtilisin domain. Trp106 and Trp113 are on one of the α-helices. Therefore, the alterations would lead to the alteration of Trp106 and Trp113. As studies on subtilisin E [24], G34A and G35A have a blue shift in fluorescence spectra.

A single Ala substitution of these residues affected the subtilisin conformation (**Fig. 3**) and caused an ~10-fold reduction in the catalytic efficiency (**Table 1**). The double Ala substitution mutant, Y10A/G35A, had a dramatically altered conformation (**Fig. 4**) and showed a significant loss (3–4 orders of magnitude) of catalytic efficiency (**Table 1**). Furthermore, maturation of the quadruple Ala substitution mutant, Y10A/G13A/G34A/G35A, was blocked during precursor folding *in vivo*. These results revealed that these multi-site mutations would result in a loss of the chaperone function for the propeptide. In addition, it seems that these hydrophobic residues cooperate for the chaperone function of the propeptide.

Generally, mutants have a lower α-helix content than WT protein. As the study on subtilisin E [24], decrease in the α-helix content of subtilisin could be due to loosening of the secondary structure. However, G13A and G35A have increased helical contents that would lead to an altered structure of IMC. This result is similar to that of a mutant of cucumisin (Y37A) [25]. To explain this phenomenon clearly, further structural studies are needed.

It is interesting to note that the yield of active subtilisin could be determined by the interaction between the propeptide and the subtilisin domains and the catalytic efficiency of mature subtilisin, such as ΔN15, Y10A/G13A/G35A, and Y10A/G13A/G34A/G35A. During the precursor folding, mutation of essential residues on the propeptide alters the formation of some hydrogen bonds, which are necessary for the maturation of active subtilisin. Therefore, conformation change would alter the catalytic efficiency and lower the yield of active subtilisin.

Supplementary Data

Supplementary data are available at *ABBS* online.

Funding

This work was supported by a grant from the Research Foundation for Youth Scholars of Beijing Technology and Business University (No. QNJJ2014-24).

References

1. Anfinsen CB. Principles that govern the folding of protein chains. Science 1973, 181: 223–230.
2. Shinde U and Inouye M. Intramolecular chaperones: polypeptide extensions that modulate protein folding. Semin Cell Dev Biol 2000, 11: 35–44.
3. Yabuta Y, Takagi H, Inouye M and Shinde U. Folding pathway mediated by an intramolecular chaperone: propeptide release modulates activation precision of pro-subtilisin. J Biol Chem 2001, 276: 44427–44434.
4. Baker D, Sohl JL and Agard DA. A protein-folding reaction under kinetic control. Nature 1992, 356: 263–265.
5. Winther JR and Sorensen P. Propeptide of carboxypeptidase Y provides a chaperone-like function as well as inhibition of the enzymatic activity. Proc Natl Acad Sci USA 1991, 88: 9330–9334.
6. Inouye M. Intramolecular chaperone: the role of the propeptide in protein folding. Enzyme 1991, 45: 314–321.
7. Jia Y, Liu H, Bao W, Weng M, Chen W, Cai Y and Zheng Z, *et al*. Functional analysis of propeptide as an intramolecular chaperone for

in vivo folding of subtilisin nattokinase. FEBS Lett 2010, 584: 4789–4796.
8. Shinde UP, Liu JJ and Inouye M. Protein memory through altered folding mediated by intramolecular chaperones. Nature 1997, 389: 520–522.
9. Thomas PJ, Qu BH and Pedersen PL. Defective protein folding as a basis of human disease. Trends Biochem Sci 1995, 20: 456–459.
10. Inouye M, Fu X and Shinde U. Substrate-induced activation of a trapped IMC-mediated protein folding intermediate. Nat Struct Biol 2001, 8: 321–325.
11. Bryan P, Wang L, Hoskins J, Ruvinov S, Strausberg S, Alexander P and Almog O, *et al*. Catalysis of a protein folding reaction: mechanistic implications of the 2.0 Å structure of the subtilisin–prodomain complex. Biochemistry 1995, 34: 10310–10318.
12. Jain SC, Shinde U, Li Y, Inouye M and Berman HM. The crystal structure of an autoprocessed Ser221Cys-subtilisin E-propeptide complex at 2.0 Å resolution. J Mol Biol 1998, 284: 137–144.
13. Zheng ZL, Zuo ZY, Liu ZG, Tsai KC, Liu AF and Zou GL. Construction of a 3D model of nattokinase, a novel fibrinolytic enzyme from Bacillus natto. A novel nucleophilic catalytic mechanism for nattokinase. J Mol Graph Model 2005, 23: 373–380.
14. Zheng ZL, Ye MQ, Zuo ZY, Liu ZG, Tai KC and Zou GL. Probing the importance of hydrogen bonds in the active site of the subtilisin nattokinase by site-directed mutagenesis and molecular dynamics simulation. Biochem J 2006, 395: 509–515.
15. Weng M, Zheng Z, Bao W, Cai Y, Yin Y and Zou G. Enhancement of oxidative stability of the subtilisin nattokinase by site directed mutagenesis expressed in *Escherichia coli*. Biochim Biophys Acta 2009, 1794: 1566–1572.
16. Sumi H, Hamada H, Tsushima H, Mihara H and Muraki H. A novel fibrinolytic enzyme in the vegetable cheese natto: a typical and popular soybean food in the Japanese diet. Experientia 1987, 43: 1110–1111.
17. Yanagisawa Y, Chatake T, Naito S, Ohsugi T, Yatagai C, Sumi H and Kawaguchi A. X-ray structure determination and deuteration of nattokinase. J Synchrotron Radiat 2013, 20: 875–879.
18. Sumi H, Hamada H, Nakanishi K and Hiratani H. Enhancement of the fibrinolytic activity in plasma by oral administration of nattokinase. Acta Haematol 1990, 84: 139–143.
19. Ho SN, Hunt HD, Horton RM, Pullen JK and Pease LR. Site-directed mutagenesis by overlap extension using the polymerase chain reaction. Gene 1989, 77: 51–59.
20. Studier FW, Rosenberg AH and Dunn JJ. Use of T7 RNA polymerase to direct expression of cloned genes. Methods Enzymol 1990, 185: 60–89.
21. Laemmli UK. Cleavage of structural proteins during the assembly of the head of bacteriophage T4. Nature 1970, 227: 680–685.
22. Carter P and Wells JA. Dissecting the catalytic triad of a serine protease. Nature 1988, 332: 564–568.
23. Chen YH, Yang JT and Martinez HM. Determination of the secondary structures of proteins by circular dichroism and optical rotatory dispersion. Biochemistry 1972, 11: 4120–4131.
24. Sone M, Falzon L and Inouye M. The role of tryptophan residues in the autoprocessing of prosubtilisin E. Biochim Biophys Acta 2005, 1749: 15–22.
25. Nakagawa M, Ueyama M, Tsuruta H, Uno T, Kanamaru K, Mikami B and Yamagata H. Functional analysis of the cucumisin propeptide as a potent inhibitor of its mature enzyme. J Biol Chem 2010, 285: 29797–29807.